Functionalized Graphene Oxide in Enzyme Engineering: A Selective Modulator for Enzyme Activity and Thermostability

Liling Jin,[†] Kai Yang,[†] Kai Yao,[†] Shuai Zhang,[†] Huiquan Tao,[†] Shuit-Tong Lee,[†,‡] Zhuang Liu,[†,*] and Rui Peng[†,*]

[†]Institute of Functional Nano & Soft Materials (FUNSOM), Jiangsu Key Laboratory for Carbon-Based Functional Materials & Devices, Soochow University, Suzhou, Jiangsu 215123, China and [‡]Center of Super-Diamond and Advanced Films (COSDAF), Department of Physics and Materials Science, City University of Hong Kong, Hong Kong SAR, China

ABSTRACT The understanding of interactions between nanomaterials and biomolecules is of fundamental importance to the area of nanobiotechnology. Graphene and its derivative, graphene oxide (GO), are two-dimensional (2-D) nanomaterials with interesting physical and chemical properties and have been widely explored in various directions of biomedicine in recent years. However, how functionalized GO interacts with bioactive proteins such as enzymes and its potential in enzyme engineering have been rarely explored. In this study, we carefully investigated the interactions between serine proteases and GO functionalized with different amine-terminated polyethylene glycol (PEG). Three well-characterized serine proteases (trypsin, chymotrypsin, and proteinase K) with important biomedical and industrial applications were analyzed. It is found that these PEGylated GOs could selectively improve trypsin activity and thermostability (60−70% retained activity at 80 °C), while exhibiting barely any effect on chymotrypsin or proteinase K. Detailed investigation illustrates that the PEGylated GO-induced acceleration is substrate-dependent, affecting only phosphorylated protein substrates, and that at least up to 43-fold increase could be achieved depending on the substrate concentration. This unique phenomenon, interestingly, is found to be attributed to both the terminal amino groups on polymer coatings and the 2-D structure of GO. Moreover, an enzyme-based bioassay system is further demonstrated utilizing our GO-based enzyme modulator in a proof-of-concept experiment. To our best knowledge, this work is the first success of using functionalized GO as an efficient enzyme positive modulator with great selectivity, exhibiting a novel potential of GO, when appropriately functionalized, in enzyme engineering as well as enzyme-based biosensing and detection.

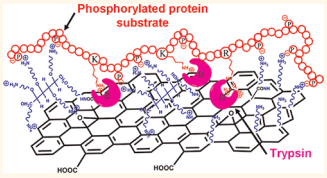

KEYWORDS: graphene oxide · nano-bio interfaces · enzyme engineering · serine protease · trypsin

Enzymes are biomacromolecules (usually proteins) that catalyze chemical and biochemical reactions. They play indispensable roles in living organisms, regulating almost all chemical reactions involved in numerous biological processes, such as signal transduction, gene expression, immune responses, metastasis, and metabolism. Other than their *in vivo* roles, enzymes are widely used in pharmaceutical and medical fields, food and environmental industry, biofuel area, as well as life science studies.[1,2] Therefore, regulation of enzyme activity and stability is very important and has always attracted great attention. Various enzyme regulators, ranging from proteins, peptides, and synthetic organic molecules, have been discovered. Recently, nanomaterials evolve as promising alternatives for enzyme modulation. Nanomaterials provide large surface areas for biomolecule adsorption and can be engineered to present multiple surface functional groups for interacting with biomolecules, such as enzymes and/or their substrates. Several types of nanomaterials, including gold nanoparticles,[3−5] magnetite nanoparticles,[6] alumina nanoparticles,[7,8] and porous silica structures,[9−11] have been reported to show positive effects on enzymes, yet mostly through enzyme immobilization process.[12,13]

In the past few years, graphene and its water-soluble derivative, graphene oxide (GO), have attracted huge attention owing to their interesting physical and chemical properties and shown wide applications in various fields including biotechnology and biomedicine.[14−17] GO, in particular, possesses a single-layered, two-dimensional (2-D), sp^2 hybrid structure with sufficient surface groups, offering a unique double-sided, easily accessible substrate for multivalent functionalization and efficient loading of molecules from small organic ones to biomacromolecules. We and other groups have already shown the potential of functionalized GO in gene and drug delivery,[18−24] cellular imaging,[25,26] cancer therapeutics,[27−35] biosensing,[36−41] as well as antibacterial agent.[42,43] The toxicology of GO and its derivatives has

* Address correspondence to rpeng@suda.edu.cn, zliu@suda.edu.cn.

Received for review January 16, 2012 and accepted May 10, 2012.

Published online May 10, 2012
10.1021/nn300217z

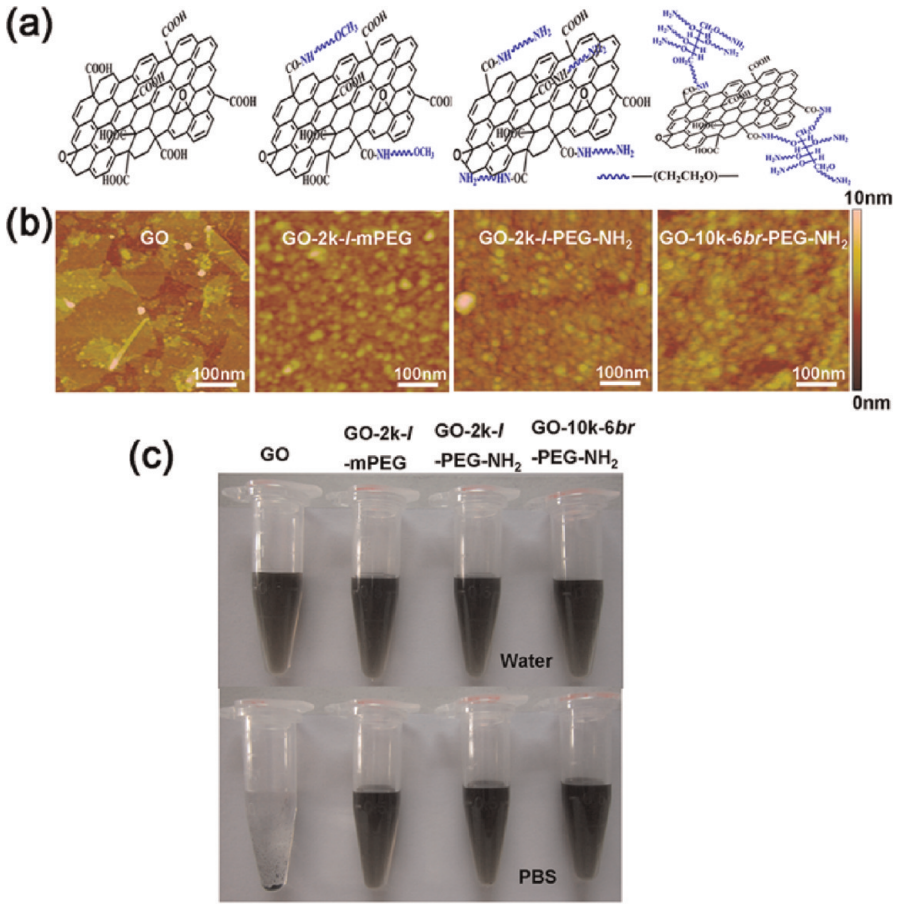

Figure 1. GO nanosheets used in the study: schemes (a), AFM images (b), and dispersibility in water and PBS (c) of GO, GO-2k-*l*-mPEG, GO-2k-*l*-PEG-NH_2, and GO-10k-6*br*-PEG-NH_2. Photo in (c) was taken after the solutions (0.08 mg/mL) were centrifuged at 21 000*g* for 5 min.

also been reported in a number of *in vitro* and *in vivo* studies, suggesting that the toxicity of GO is closely associated with its surface coatings and sizes.[44−48] Regarding the interactions between GO and biomacromolecules, such as enzymes, GO has been reported in a few studies, mostly for biosensing, as a matrix for immobilization of several enzymes, including glucose oxidase,[49−52] horseradish peroxidase,[53−57] and hemoglobin.[58] In a recent work, De *et al.* uncovered that the activity of chymotrypsin could be strongly inhibited by addition of as-made GO.[59] However, for further exploration and better optimization of GO-based nanomedicine and nanobiotechnology, one critical and fundamental question still needs to be addressed yet has been insufficiently studied thus far, that is, the detailed effects of GO, especially its functionalized derivatives, on active biomolecules such as enzymes and proteins. Intensive work to investigate such effects and interactions, as well as to understand their regulating factors, is therefore of great importance and highly desirable.

In this study, we started to explore the interactions between functionalized GO and serine proteases, a large family of enzymes with important biomedical and industrial applications.[2] Three well-characterized serine proteases (trypsin,[60] chymotrypsin,[61] and proteinase K[62]) with important biomedical and industrial applications were chosen as models. GO conjugated with two types of amine-terminated PEGs, 2 kDa PEG-diamine (2k-*l*-NH_2-PEG-NH_2) and 10 kDa amine-terminated six-arm-branched PEG (10k-6*br*-PEG-NH_2), were used in our experiments. Interestingly, we found that both types of PEGylated GOs (GO-2k-*l*-PEG-NH_2 and GO-10k-6*br*-PEG-NH_2) were able to selectively improve the activity and thermostability of trypsin, while exhibiting barely any effect on chymotrypsin or proteinase K. Further analysis showed that the improved trypsin activity was substrate-dependent, affecting only phosphorylated protein substrates. A series of subsequent investigations revealed the involving factors as both the terminal NH_2 groups on PEG coatings and the unique 2-D structure of GO. To our best knowledge, this is the first report of using functionalized GOs as efficient enzyme positive modulators while, more interestingly, exhibiting great selectivity for their target enzyme/substrate pair.

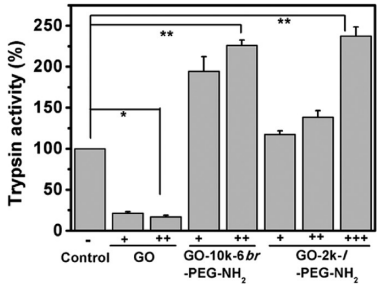

Figure 2. Effects of GO nanosheets with different surface modifications on trypsin activity. Trypsin was incubated with increasing concentrations of GO, GO-10k-6*br*-PEG-NH_2, and GO-2k-*l*-PEG-NH_2, followed by enzymatic analysis using casein as the substrate. As a control, GO nanosheets were substituted by water. +, ++, and +++ represent 30, 40, and 80 μg/mL of GO nanosheets in the analysis reactions, respectively. Error bars represent the standard deviation ($n \geq 3$). *P < 0.000001, **P < 0.00002.

RESULTS AND DISCUSSION

Preparation and Functionalization of GO Nanosheets. GO was prepared from graphite as previously described.[33] Differently, PEGylated GO nanosheets (GO-2k-*l*-PEG-NH_2 and GO-10k-6*br*-PEG-NH_2) were prepared from GO sheets by covalent conjugation with 2 kDa PEG-diamine (2k-*l*-NH_2-PEG-NH_2) and 10 kDa amine-terminated six-arm-branched PEG (10k-6*br*-PEG-NH_2) *via* amide formation (Figure 1a), respectively, and confirmed by infrared (IR) spectra (Supporting Information, Figure S1). Atomic force microscope (AFM) images showed that both types of PEGylated GO were mostly single- or double-layered ultrasmall nanosheets with a size range of 10−50 nm (Figure 1b). Highly improved dispersibility in physiological solutions was achieved after PEGylation, without showing any noticeable aggregation in PEGylated GO samples after being centrifuged in phosphate buffered saline (PBS) at 21 000*g* for 5 min (Figure 1c).

Substrate-Dependent Effects of PEGylated GO Nanosheets on Trypsin Activity. The effects of GO with or without PEGylation on trypsin activity were first analyzed using a general trypsin substrate casein. As shown in Figure 2, without PEGylation, as-made GO significantly inhibited enzyme activity, similar to the results in a previous report.[59] This is understandable and likely due to the nonspecific binding of enzyme proteins on GO *via* hydrophobic interactions. The active center in the enzyme is then blocked or denatured, leading to the dramatically decreased enzyme activity. Interestingly, incubation of GO-2k-*l*-PEG-NH_2 and GO-10k-6*br*-PEG-NH_2 with trypsin showed no inhibitory effects at all, but rather strongly accelerated the digestion of casein in a concentration-dependent manner. No hydrolysis of casein was detected when the two types of PEGylated GOs were incubated with casein in the absence of trypsin (Supporting Information Figure S2 and data not shown), suggesting that the observed higher digestion efficiency is attributed to the enhanced trypsin activity by PEGylated GO nanosheets. In addition, GO-10k-6*br*-PEG-NH_2 showed a much higher ability for activity enhancement than GO-2k-*l*-PEG-NH_2 under the same concentrations.

TABLE 1. Effects of PEGylated GO Nanosheets on Trypsin Digestion of Different Substrates[a]

substrate	functionalized GO nanosheets	concentrations of GO(μg/mL)	trypsin activity (%)
TAME	GO-10k-6*br*-PEG-NH_2	40	81.7 ± 8
	GO-2k-*l*-PEG-NH_2	80	78 ± 11
Hb	GO-10k-6*br*-PEG-NH_2	40	95.6 ± 3.4
	GO-2k-*l*-PEG-NH_2	80	108 ± 2
BSA	GO-10k-6*br*-PEG-NH_2	40	100 ± 5.6
	GO-2k-*l*-PEG-NH_2	80	97 ± 4.9

[a] Trypsin activity (%) in each reaction was normalized to that in the corresponding control reaction.

We next tested the effects of these PEGylated GO nanosheets on trypsin activity using three different substrates: two protein substrates hemoglobin (Hb) and bovine serum albumin (BSA), as well as a small molecule substrate N_α-*p*-tosyl-L-arginine methyl ester hydrochloride (TAME). However, different from the casein case, both PEGylated GO nanosheets showed barely any effect on the digestion of either Hb or BSA by trypsin and even slight inhibitory effects on the hydrolysis of TAME (Table 1), suggesting that they are able to affect the activity of trypsin in a substrate-dependent manner.

Specific Enhancement in Trypsin Digestion of Phosphoproteins by PEGylated GO Nanosheets. Since casein is a family of phosphoproteins while Hb and BSA are not, we next investigated whether substrate phosphorylation played a role in the observed activity enhancement by PEGylated GO nanosheets. Native whole casein consists of three major members that can be distinguished by electrophoresis: α-casein, β-casein, and κ-casein.[63] Whole casein and dephosphorylated whole casein (decasein) were subjected to trypsin digestion in the presence and absence of GO-2k-*l*-PEG-NH_2 or GO-10k-6*br*-PEG-NH_2, and digestion products as well as undigested substrates remaining in each reaction at different time intervals (3 and 4 min) were separated by sodium dodecyl sulfate polyacrylamide gel electrophoresis (SDS-PAGE) followed by Coomassie Blue stain. Dephosphorylation caused band shifts of α- and β-casein to lower positions (Figure 3a, de-α- and de-β-casein). A faint shifted band was detected for κ-casein, probably due to inefficient dephosphorylation by alkaline phosphatase. Consistent with results shown in Figure 2, casein was digested much faster in the presence of GO-2k-*l*-PEG-NH_2 or GO-10k-6*br*-PEG-NH_2, as evidenced by the much fainter bands of undigested remains at both time intervals (Figure 3b, compare lane 5, lane 7 with lane 3, α- and β-casein; Figure 3d, columns in pink), whereas decasein was

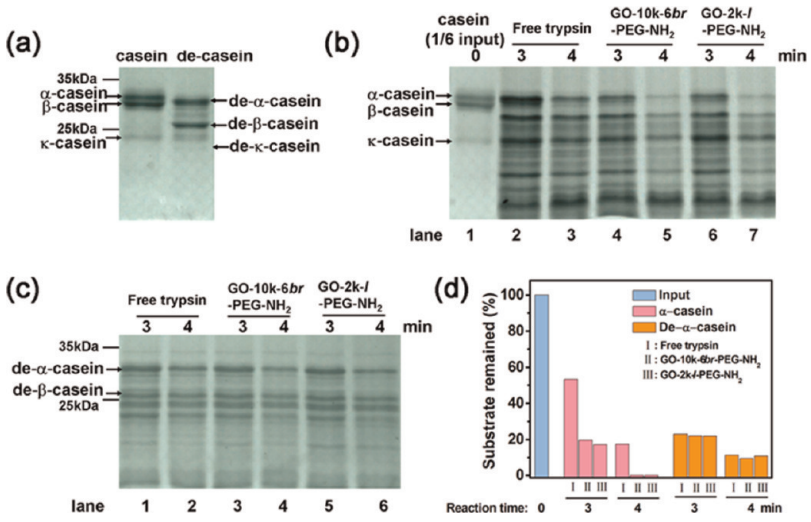

Figure 3. Specific acceleration of trypsin digestion of phosphoproteins by PEGylated GO. (a) Whole casein and dephosphorylated whole casein (decasein) separating on 12% SDS-PAGE followed by Coomassie Blue stain. (b,c) Time course of trypsin digestion of whole casein (b) and decasein (c) in the absence or presence of GO-2k-*l*-PEG-NH_2 or GO-10k-6*br*-PEG-NH_2. The digestion reactions were stopped at different time intervals (3 and 4 min), and the digestion products as well as undigested substrates remaining in each reaction were separated on 12% SDS-PAGE followed by Coomassie Blue stain. Positions of full-length α-casein, β-casein, κ-casein, de-α-casein, de-β-casein, and possible de-κ-casein are indicated by arrows. All other bands were digestion products. (d) Quantification of the percentage of undigested remains of α-casein and de-α-casein from (b) and (c).

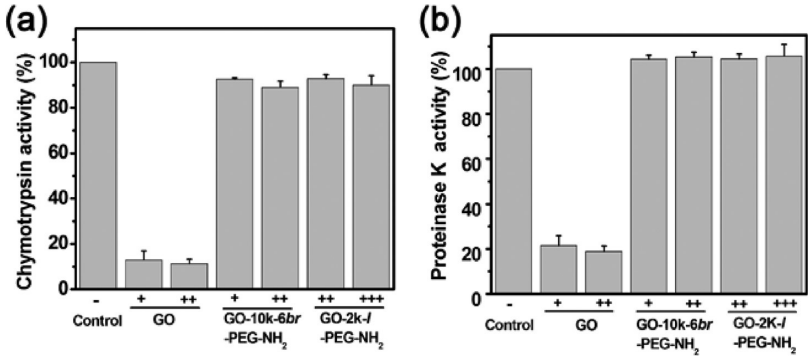

Figure 4. Effects of GO nanosheets with different surface modifications on chymotrypsin (a) and proteinase K (b) activities. The indicated enzyme (chymotrypsin or proteinase K) was incubated with increasing concentrations of GO, GO-2k-*l*-PEG-NH_2, and GO-10k-6*br*-PEG-NH_2, followed by enzymatic analysis using casein as the substrate. As a control, GO nanosheets were substituted by water; +, ++, and +++ represent 30, 40, and 80 μg/mL of GO nanosheets in the analysis reactions, respectively. Error bars represent the standard deviation ($n \geq 3$).

digested in relatively similar rates regardless of PEGylated GO addition (Figure 3c, compare lane 4, lane 6 with lane 2; Figure 3d, columns in orange). The observed quicker disappearance of α- and β-casein was not due to possible adsorption of them onto PEGylated GO since, in mock reactions (Supporting Information Figure S2), the SDS-PAGE sample preparation using 2 X Laemmli buffer[64] before electrophoresis abolished all protein interactions as well as any possible protein–GO interactions. Although digestion of κ-casein and de-κ-casein was hard to analyze due to the interference from partially digested casein members, the results obtained from α- and β-casein clearly demonstrated that both PEGylated GO nanosheets could specifically accelerate trypsin digestion of phosphorylated protein substrates.

Effects of PEGylated GO Nanosheets on Other Serine Proteases. Trypsin belongs to the serine protease family, a large family of enzymes that represents almost one-third of the known proteases and performs a variety of critical physiological and cellular functions.[65] Therefore, the effects of GO-2k-*l*-PEG-NH_2 and GO-10k-6*br*-PEG-NH_2 on other serine protease activities were analyzed, as well. Two typical serine proteases with similar catalytic mechanisms to trypsin were investigated: chymotrypsin from the same subfamily as trypsin (chymotrypsin-like serine protease),[65] and proteinase K from subtilisin-like subfamily.[62] As shown in Figure 4, both GO-2k-*l*-PEG-NH_2 and GO-10k-6*br*-PEG-NH_2 slightly impeded the digestion of casein by chymotrypsin (less than 10%), while it had little if any effect on proteinase K activity, indicating that the stimulatory effect on

TABLE 2. Zeta-Potentials of GO and Differently Functionalized GO Nanosheets Used in Figure 5a

sample	GO	GO-10k-6*br*-PEG-NH_2	GO-10k-6*br*-PEG-NH_2-AA	GO-2k-*l*-PEG-NH_2	GO-2k-*l*-mPEG
zeta-potential	-40.2 ± 3.68	-8.67 ± 0.477	-26.8 ± 1.27	-28.6 ± 1.20	-33.0 ± 3.26

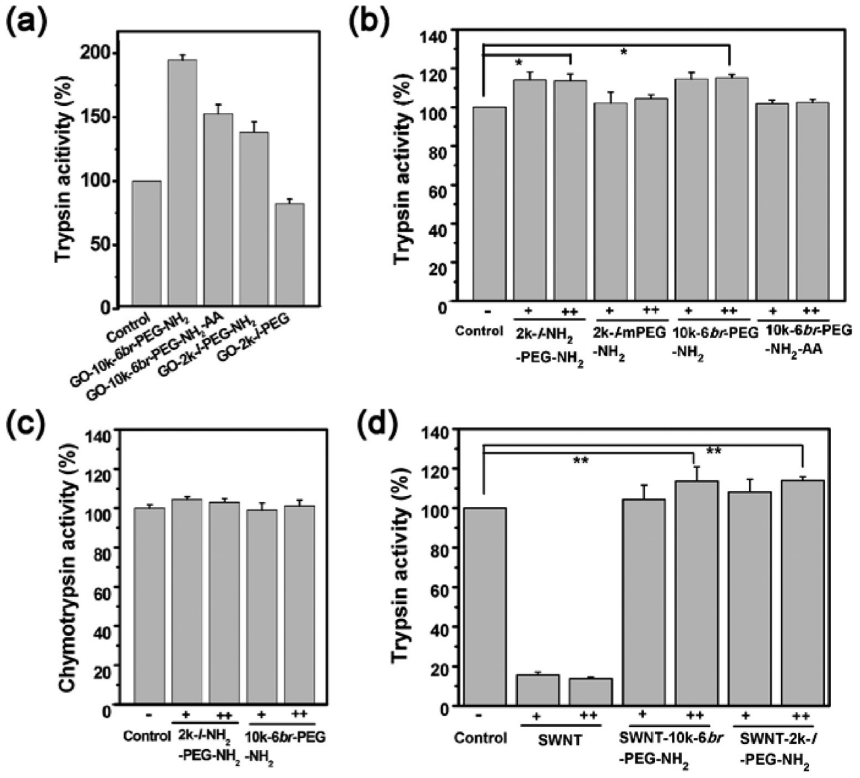

Figure 5. Involvement of functional groups and the structure of sp^2 nanomaterials in the selective stimulation of trypsin. Trypsin treated by PEGylated GO nanosheets with different functional groups as indicated in the text (a), the corresponding PEG polymers (b), or PEGylated SWNTs (d), and chymotrypsin treated by PEG polymers (c) were subjected to enzymatic analysis using casein as the substrate. The GO concentration in (a) was 30 μg/mL. Materials concentrations in (b−d): + and ++ represent 150 and 200 μg/mL for PEGs (b,c), while 30 and 40 μg/mL for oxidized SWNTs (d), respectively. Error bars represent the standard deviation ($n \geq 3$). *$P < 0.001$, **$P < 0.05$.

trypsin is not a general phenomenon for all serine proteases, even those who share very similar catalytic mechanisms. Since chymotrypsin and trypsin are closely related to each other with a high degree of similarity in their primary amino acid sequences and overall tertiary structures,[66,67] their distinct responses to PEGylated GO nanosheets suggest a high possibility that the PEGylated GO-mediated activity enhancement may be trypsin-specific.

Dissecting the Functional Elements of PEGylated GO Nanosheets Involved in Trypsin Activity Stimulation. Surface modification of nanomaterials normally alters the existing surface functional groups and/or introduces new ones, thus enabling enhanced or even new properties and/or functions. The opposite effects of GO and PEGylated GO nanosheets on trypsin activity suggest an important contribution from the PEGylation, which altered the nano-bio interfaces and could affect protein binding. We next wondered if the amino groups on PEG coatings would affect the specific enzyme stimulatory capability of PEGylated GO. Acetic anhydride (AA) was incubated with GO-10k-6*br*-PEG-NH_2 to block its NH_2 groups. Given the poor solubility of GO-10k-6*br*-PEG-NH_2 in organic solvents, the blocking reaction had to be carried out in the aqueous phase, resulting in only partial blocking of amino groups. Nevertheless, partially blocked GO-10k-6*br*-PEG-NH_2 (GO-10k-6*br*-PEG-NH_2-AA), as evidenced by its zeta-potential dropping to between those of GO and GO-10k-6*br*-PEG-NH_2 (Table 2), was able to enhance trypsin activity, but with a 40% decrease in efficiency (Figure 5a) when compared with unblocked GO-10k-6*br*-PEG-NH_2, correlating well with the zeta-potential data.

Given the low blocking efficiency, another approach was employed. The same method for preparing GO-2k-*l*-PEG-NH_2 was used to conjugate 2 kDa monoamine-terminated PEG (2k-*l*-mPEG-NH_2) to GO nanosheets, obtaining GO-2k-*l*-mPEG, which contains no free amino groups. Compared to GO-2k-*l*-PEG-NH_2, GO-2k-*l*-mPEG completely lost the ability to enhance

trypsin activity (Figure 5a), further implicating the involvement of amino groups.

Since these functional amino groups are not directly conjugated to the GO surface, but present on PEG coatings, one question arises as to whether the observed strong stimulatory effect on trypsin activity is really a novel function of PEGylated GO, or merely the intrinsic properties of the two NH_2-PEG polymers. To address this question, equivalent amounts of 2k-*l*-NH_2-PEG-NH_2 and 10k-6*br*-PEG-NH_2 as used in the preparation of NH_2-PEGylated GO nanosheets were incubated with trypsin, and their effects on trypsin activity were analyzed. As shown in Figure 5b, both 2k-*l*-NH_2-PEG-NH_2 and 10k-6*br*-PEG-NH_2 were able to increase the trypsin digestion of casein by 15% ($P < 0.001$). Again, 10k-6*br*-PEG-NH_2-AA was prepared by incubating 10k-6*br*-PEG-NH_2 with AA, except this time in dichloromethane to enhance the blocking efficiency. Neither 10k-6*br*-PEG-NH_2-AA nor 2k-*l*-mPEG-NH_2 exhibited any effect on trypsin activity. Taken together, the results show that the two coating polymers, 2k-*l*-NH_2-PEG-NH_2 and 10k-6*br*-PEG-NH_2, can in fact act through their amino groups to enhance trypsin activity by themselves, but only to a rather limited extent, much lower than that of PEGylated GO. In addition, the fact that these two NH_2-PEG polymers had little effect on the digestion of casein by chymotrypsin (Figure 5c) indicates that they might be responsible for the observed specificity toward trypsin rather than chymotrypsin.

Although unmodified GO showed strong inhibitory effect on trypsin activity, the different levels of enhancement by PEGylated GO and NH_2-PEG polymers imply certain involvement of GO nanosheets. This is also suggested by the fact that SWNT-10k-6*br*-PEG-NH_2, prepared by substitution of 2-D GO nanosheets with 1-D oxidized SWNTs, was able to enhance trypsin activity only to an extent similar to that of 10k-6*br*-PEG-NH_2 (Figure 5d).

Specific Protection of Trypsin against Thermal Denaturation by PEGylated GO. We further analyzed the effects of PEGylated GO on the thermostability of trypsin. As shown in Figure 6a, when incubated with trypsin at high temperatures (70 and 80 °C), both GO-2k-*l*-PEG-NH_2 and GO-10k-6*br*-PEG-NH_2 were able to efficiently protect trypsin from thermal denaturation above 70 °C, while coating polymers alone (2k-*l*-NH_2-PEG-NH_2 and 10k-6*br*-PEG-NH_2) showed little protection. Since we have shown that PEGylated GO can enhance trypsin activity, to ensure the observed high retention of trypsin activity truly represents the result of protection, a series of control experiments were performed, where trypsin was heat denatured first, then its retaining activity was analyzed in the presence of either PEGylated GO or NH_2-PEG polymers (Figure 6b). None of them was able to rescue the enzymatic activity after denaturation, proving that the two types of PEGylated GO can indeed interact with trypsin and greatly

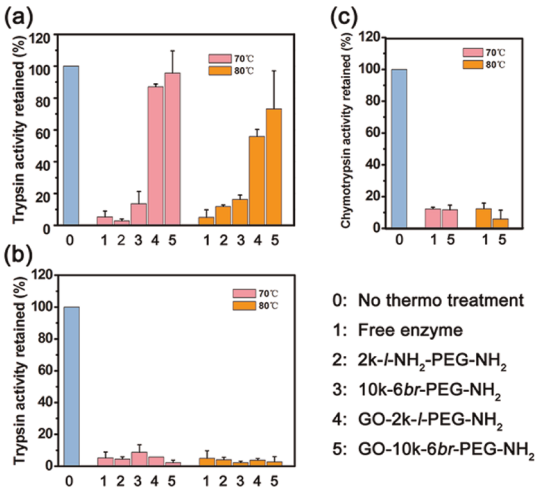

Figure 6. Specific thermal protection of trypsin by PEGylated GO nanosheets. PEGylated GO nanosheets (40 μg/mL) or the corresponding NH_2-PEG polymers (200 μg/mL) were added to trypsin solution before (a) or after (b) thermal denaturation at indicated temperatures for 5 min, and the retaining enzymatic activity was analyzed using casein as the substrate. (c) PEGylated GOs (40 μg/mL) were added to chymotrypsin solution before thermal denaturation at indicated temperatures for 5 min, and the retained enzymatic activity was analyzed using casein as the substrate. Error bars represent the standard deviation ($n \geq 3$).

enhance its thermostability. Similar to the stimulatory effect on trypsin activity, this thermal protection is also specific for trypsin, not for chymotrypsin (Figure 6c). Despite that, they are two independent events, demonstrated by the overall protection of trypsin against heat denaturation regardless of the substrates used in subsequent enzymatic activity analysis (Figure 6a and Supporting Information Figure S3).

Enzyme Kinetics Analysis and a Hypothesis of the Stimulatory Effect of PEGylated GO on Trypsin. We have shown that two types of PEGylated GO, GO-2k-*l*-PEG-NH_2 and GO-10k-6*br*-PEG-NH_2, can interact with trypsin, efficiently protecting it from thermal denaturation up to 80 °C and selectively accelerating the digestion rate of highly phosphorylated protein substrates. Although the exact mechanism of how PEGylated GOs interact with trypsin and function as its thermal stabilizer remains to be discovered at this point, we engaged a series of enzyme kinetics analysis to investigate how they act as a selective accelerator for highly phosphorylated substrates.

Trypsin specifically cleaves peptide chains after lysine (Lys) and arginine (Arg), two amino acids commonly found in proteins. Therefore, the digestion of protein substrates by trypsin is usually not an idealized single-substrate reaction, but rather a complex reaction involving multiple cleavage sites flanked by various amino acid sequences that generate various microenvironments, and also a multistep process which results in a number of smaller peptide fragments appearing as both the intermediates and products. Nevertheless, we started to investigate the effect of

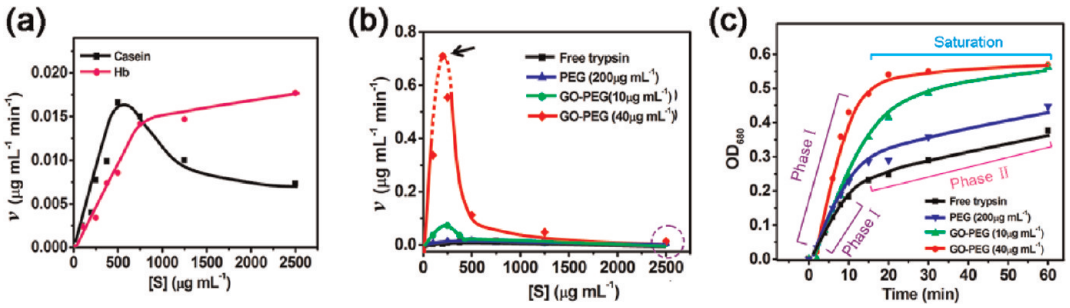

Figure 7. Enzyme kinetic analysis of trypsin. (a) Effects of substrate concentration ([S]) on the initial velocity (*v*) of trypsin digestion (*v* by [S] plot). The progress curve (every 5−15 s) of each digestion of casein (black) or Hb (orchid) of indicated concentrations was recorded for *v* measurement. (b) Plot of *v* by [S] of trypsin digestion of casein in the absence or presence of indicated concentrations of 10k-6*br*-PEG-NH_2 or GO-10k-6*br*-PEG-NH_2 (abbreviated as PEG and GO-PEG in this figure, respectively). The red dashed line represents an uncertain portion of the curve, due to the fact that the corresponding reaction (200 μg/mL casein as substrate, black arrow) was completed within the first few seconds, making it almost impossible for accurate *v* measurement. (c) Progress curves (0−60 min) of reactions containing 2500 μg/mL casein as substrate (dashed circle in (b)). The amount of products was analyzed by Lowry assay as usual and represented by OD_{680}.

substrate concentration (denoted as [S]) on the initial velocity (*v*) of the digestion, a classical kinetics analysis. As shown in the velocity curve as a function of [S] (*v* by [S] plot, Figure 7a), for trypsin digestion of Hb, *v* increased with increasing Hb concentrations. In contrast, for digestion of casein, the highly phosphorylated substrates, the velocity curve rose to a peak and then declined as casein concentration increased, resembling the kinetics of substrate inhibition, a common phenomenon occurring in about 20% of enzymes,[68,69] and indicating casein as an inhibitory substrate for trypsin. In the substrate recognition step before the cleavage, the positively charged side chains of Lys and Arg must be attracted to the "catalytic pocket" (S1 pocket) of trypsin through electrostatic interaction with the negatively charged aspartic acid (Asp) located at the bottom of S1.[70,71] Therefore, the negative charges of phosphate groups on phosphoprotein substrates (*e.g.*, casein) would impair the binding of Lys/Arg to the S1 pocket and thus might in turn cause the observed inhibitory effect at higher [S].

The presence of high concentration 10k-6*br*-PEG-NH_2 in the trypsin digestion of casein only slightly increased the reaction *v* (Figure 7b, blue line). Addition of GO-10k-6*br*-PEG-NH_2 in the reaction, on the other hand, dramatically increased the velocity at low [S] (5- and 43-fold increase at the peak value for 10 and 40 μg/mL GO-10k-6*br*-PEG-NH_2, respectively), but to our surprise, both curves rapidly declined after rising to the peak as [S] went up, suggesting a significant substrate inhibition effect (Figure 7b). Since our previous results (Figures 2, 3, and 5) were all carried out at 2500 μg/mL casein concentration, we apparently very much underestimated the stimulatory effect of PEGylated GO. It is worth noting that for the reaction containing 200 μg/mL casein as substrate (Figure 7b, black arrow), its *v* was almost impossible to be accurately measured due to rapid completion of the reaction within the first few seconds in the presence of 40 μg/mL GO-10k-6*br*-PEG-NH_2. Therefore, a conservative estimate would be that at least up to 43-fold acceleration induced by PEGylated GO could be achieved depending on the substrate concentration.

We further explored the multistep reaction kinetics by analyzing the progress curve over 0−60 min period. For the trypsin reaction, two phases with distinct slopes (average reaction rates) were observed while the substrate was still at saturating levels (Figure 7c, black line), and the reaction switched to a slower rate (about 20% of that in phase I) when entering phase II. One plausible explanation is that these two phases probably reflect another aspect of the enzyme−substrate recognition during the process. At the early stage of digestion (phase I), a long peptide chain with multiple cleavage sites would favor the recognition of neighboring sites by the enzyme finishing the previous round of cleavage. The length of peptide intermediates shortens as the reaction goes on, until it reaches the point that it is too short to encompass multiple sites, and the enzyme−substrate recognition will be dominated by random diffusion, resulting in a slower rate (phase II). Compared with the free trypsin reaction, a similar two-phase progress curve was recorded for the reaction with 10k-6*br*-PEG-NH_2, just exhibiting a slightly larger slope in phase I, whereas interestingly, addition of PEGylated GO in the reaction caused disappearance of the low-rate phase II, further speeding up the digestion process (Figure 7c).

After a careful comparison of the above results and those from Figures 2, 3, and 5, we came up with a hypothesis shown in Figure 8. For phosphoprotein substrates, NH_2-PEG polymers may act through their positively charged amino groups to neutralize the negative charges on the substrate and thus make it slightly more accessible to trypsin, showing a weak stimulatory effect on substrate recognition. PEGylated GO nanosheets with free amines could further amplify this effect, and the 2-D structure of GO may be unique to offer condensed and ordered PEG structures on its surface, providing a friendly nano interface for

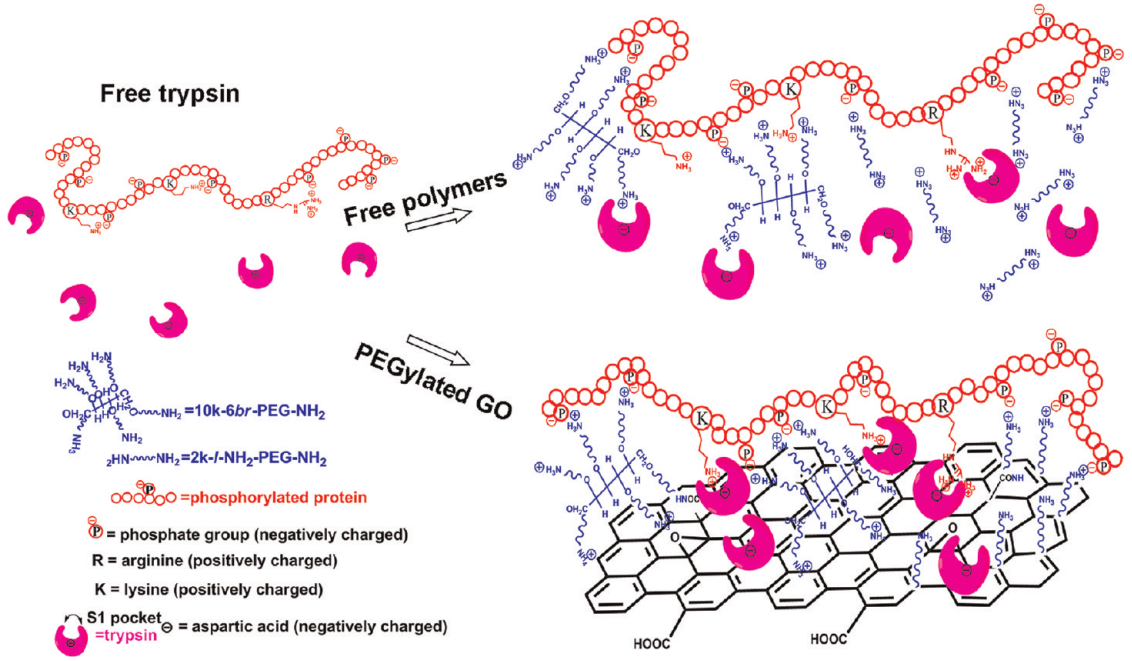

Figure 8. Schematic representation of a hypothesis that PEGylated GO nanosheets interact with trypsin and act through electrostatic interactions to facilitate phosphorylated protein substrates entering the catalytic pocket of trypsin.

interaction with both trypsin (Figure 6, by a yet unknown mechanism) as well as the substrate and later intermediates (likely through the free amines and peptide phosphate groups). Whereas for SWNTs with 1-D structure, the local PEG packing may be less condense, resulting in less effective trypsin activation.

At low [S], the packing of substrate onto PEGylated GO would help turn the recognition step into a relatively organized manner by pulling the enzyme and the substrate close to one another. As [S] increases, an increasing number of substrate molecules will be packed onto PEGylated GO. This may impair the interaction between PEGylated GO and the enzyme, resulting in the subsequent dramatic drop of *v* observed in Figure 7b. For the disappearance of phase II in PEGylated GO-assisted reaction (Figure 7c), our proposed explanation is that, during the reaction process, PEGylated GO would continue to pack generated intermediates, preventing them from releasing into the solution (free diffusion). Taken together, our kinetics assays have shed some light on the possible mechanisms, yet further work needs to be done to confirm this hypothesis.

Promising Potentials of Functionalized GO Nanosheets. Our findings demonstrated that GO nanosheets can be functionalized to serve as selective enzyme modulators, and the interactions of PEGylated GO with biomacromolecules can be regulated through and are closely associated with their surface and interface chemistry. Therefore, GO nanosheets, when appropriately designed and engineered, could be used as modulators for certain enzymes, affecting their activity and/or stability, and thus affecting the subsequent reactions. This is a novel application of GO in enzyme engineering other than enzyme immobilization and could be used to improve the selectivity and sensitivity in enzyme-based biosensing, to widen the detection condition, such as wider temperature range, or even to develop new methods for bioassays and biochemistry.

As a proof-of-concept demonstration, GO-10k-6*br*-PEG-NH_2 was explored in a simple and quick estimation of phosphoprotein contents in mixed protein samples. The design is based on the fact that addition of GO-10k-6*br*-PEG-NH_2 in trypsin proteolysis reactions will selectively accelerate the digestion of phosphoproteins, therefore, a difference in digestion rate between reactions with and without GO-10k-6*br*-PEG-NH_2 addition should be observed for phosphoprotein-containing samples. As shown in Figure 9, using this method, after a 10 min trypsin digestion, we were able to detect the presence of as low as 2% phosphoproteins in mixed samples by analyzing the digestion rates in the presence and absence of GO-10k-6*br*-PEG-NH_2, and the difference (represented by ΔOD) remained directly proportional to the phosphoprotein content in the range covering up to 100% (Figure 9 and data not shown).

In addition to the simple demonstration described above, given the important applications of trypsin in biological research and industry, the enhanced thermostability by PEGylated GO could be particularly useful since this would enable efficient selection of trypsin over other proteins and enzymes at high temperatures. For example, during the large-scale purification of trypsin from porcine or bovine pancreas, an additional short treatment of crude extracts at high

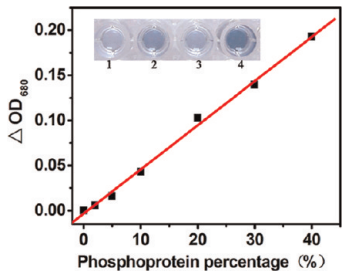

Figure 9. Detection of phosphoprotein in mixed protein samples. Samples with various phosphoprotein contents were digested by trypsin in the absence or presence of 40 μg/mL GO-10k-6*br*-PEG-NH_2 (abbreviated as GO-PEG in this figure), and the amount of digestion products were analyzed by Lowry assay as usual. For control, sample with no phosphoprotein (0%) was used. $\Delta OD = (OD_{(sample+GO\text{-}PEG)} - OD_{sample}) - (OD_{(control+GO\text{-}PEG)} - OD_{control})$. Inset: photo of four representative digestions: (1,2) samples with 5% phosphoprotein content were digested by trypsin in the absence (1) or presence (2) of GO-PEG; (3,4) samples with 40% phosphoprotein content were digested by trypsin in the absence (3) or presence (4) of GO-PEG.

temperatures in the presence of PEGylated GO could greatly promote the separation of trypsin from the extracts and enhance purification efficiency since most tissue proteins, including many pancreatic proteases that affect trypsin stability, will quickly be denatured while trypsin is protected by PEGylated GO.

Last but not the least, PEGylated GO could also be useful for other trypsin applicable and phosphoprotein-related analysis, such as mass spectrometry based phosphoproteomics,[72,73] a branch of proteomics identifying and characterizing phosphorylated proteins. Protein phosphorylation is one of the most important post-translational modifications in the cell and plays critical roles, enabling precise control and regulation of essential processes in cell cycle and differentiation. Although 30% of all cellular proteins are thought to be phosphorylated with over 500 000 estimated sites of phosphorylation,[74,75] protein phosphorylation in a living cell is often transient and dynamic, and in most cases, for a given protein, only a small portion of it is phosphorylated, resulting in the often low abundance of phosphoproteins. Therefore, enriching phosphopeptides for phosphoprotein identification and studies of phosphorylation dynamics is still a major concern in phosphoproteomics, where trypsin is the most commonly used protease in sample preparation for mass spectrometry. Addition of PEGylated GO to trypsin proteolysis reactions could selectively favor the digestion of phosphoproteins, thus enriching the low-abundant phosphopeptides for more efficient mass spectrometry identification, which in turn could promote better understanding of cellular dynamics and associated diseases.

CONCLUSION

In this study, the effects of two types of PEGylated GO nanosheets with free amines (GO-2k-*l*-PEG-NH_2 and GO-10k-6*br*-PEG-NH_2) on three important serine proteases (trypsin, chymotrypsin, and proteinase K) were investigated. Addition of either PEGylated GO nanosheets significantly improved trypsin activity and thermostability (60−70% retained activity at 80 °C), while showing barely any effect on chymotrypsin or proteinase K. Both the dephosphorylated and unphosphorylated substrates demonstrated that the improved trypsin activity is substrate-dependent, affecting only phosphorylated protein substrates. Either blocking the functional amino groups or replacing 2-D GO with 1-D SWNT abolished the stimulatory effect, suggesting the involvement of both the terminal amines on polymer coatings and the unique 2-D structure of GO. Detailed enzyme kinetics analysis revealed that PEGylated GO functions at both the initiation step and later steps along the reaction process, and that at least up to 43-fold of reaction acceleration induced by PEGylated GO could be achieved depending on the substrate concentration. On the basis of the above results, a hypothesis is proposed. Furthermore, as a proof-of-concept demonstration, a simple and fast phosphoprotein assay exploiting GO-10k-6*br*-PEG-NH_2 was developed. Although further work is required to investigate the hypothesis and the mechanism of thermostability improvement, our work highlights that the interactions of nanomaterials with biomacromolecules, in general, can be regulated through and are closely associated with their surface chemistry or nano-interfaces. Nevertheless, this is to our best knowledge the first report of functionalized GO nanosheets as efficient enzyme positive modulators with great selectivity, suggesting not only promising applications of PEGylated GO in trypsin applicable life science studies and industry, but also a great and novel potential of functionalized GO nanosheets in enzyme engineering and enzyme-based biosensing and bioassays.

EXPERIMENTAL SECTION

Reagents. 10k-6*br*-PEG-NH_2 was purchased from Sunbio Inc. (South Korea). 2k-*l*-NH_2-PEG-NH_2 and 2k-*l*-mPEG-NH_2 were purchased from Jiaxing Biomatrix Inc. (Jiaxing, China). All other reagents and enzymes were purchased from Sigma-Aldrich (St. Louis, MO, USA).

Preparation and Characterization of GO, Oxidized SWNT, PEGylated GO, and PEGylated SWNT Dispersions. GO and PEGylated GOs were prepared as previously described.[19] Briefly, GO was produced from graphite following a Hummers method with slight modifications.[76] Three types of PEGylated GOs (GO-10k-6*br*-PEG-NH_2, GO-2k-*l*-PEG-NH_2, and GO-2k-*l*-mPEG) were prepared from mixtures of 1 mg/mL GO dispersion with 5 mg/mL indicated PEG polymers. Following 55 min bath sonication (with the addition of 2 and 3 mg of *N*-(3-dimethylaminopropyl)-*N*′-ethylcarbodiimide hydrochloride (EDC) at 5 and 35 min, respectively), reactions were stirred at room temperature

for 2 h, and additional EDC was added to reach a final concentration of 1.2 mg/mL, then kept stirring for another 12 h. Excess PEG polymers were removed by filtration through Amicon Ultra centrifugal filters with molecular weight cutoff (MWCO) of 100 kDa (Millipore, Carrigtwohill, co. cork, Ireland) and repeated water washing.

Oxidized SWNTs were prepared from pristine SWNTs (Shenzhen Nsnotech Port Co. Ltd.) following the exact preparation method of GO (by $KMnO_4$, H_2O_2, and H_2SO_4) to ensure similar oxidation level to GO. PEGylated SWNTs (SWNT-2k-*l*-PEG-NH_2 and SWNT-10k-6*br*-PEG-NH_2) were prepared using oxidized SWNT and indicated PEG polymers following the exact PEGylation method of PEGylated GO as described above.

The concentrations of functionalized GOs and SWNTs were calculated using their absorbance at 230 nm (mass extinction coefficient of 65 mg mL^{-1} cm^{-1})[32] and 808 nm (mass extinction coefficient measured to be 28.4 mg mL^{-1} cm^{-1}), respectively. All functionalized GOs and SWNTs were characterized by AFM analysis using a MutiMode V AFM (Veeco), FT-IR using Hyperion series spectrometer (Bruker), and DLS on a Zen3690 (Malvern) at the scattering angle of $\theta = 17°$.

Blocking of Terminal Amino Groups. GO-10k-6*br*-PEG-NH_2 (0.2 mg/mL) was incubated with 6% AA in the reaction containing 30 mM $NaHCO_3$, 20 mM EDC, and 20 mM PBS at room temperature for 4 h. The reaction was adjusted to pH 8.0 with $NaHCO_3$, and additional EDC was added to reach a final concentration of 25 mM, followed by further incubation for 4 h. Excess AA was removed by filtration through Amicon Ultra centrifugal filters (MWCO = 100 kDa) as described above.

The terminal amino groups of 10k-6*br*-PEG-NH_2 were blocked by mixing 50 mg of 10k-6*br*-PEG-NH_2 with 2% AA and 10% pyridine in dichloromethane for 12 h. The reaction solution was blow-dried by nitrogen and then resuspended in water. Following further purification by dichloromethane extraction, dichloromethane was removed by spin-dry, and the final product 10k-6*br*-PEG-NH_2-AA was dissolved in water and freeze-dried.

Enzymatic Activity Assay. The catalytic activity of trypsin on small molecule substrate TAME (7.5 mM) was carried out using the modified spectrophotometric method as described.[77] Trypsin digestions of protein substrates, casein, Hb, and BSA (Supporting Information Table S1), were carried out as described with slight modifications.[5] Briefly, 20 μg/mL (0.86 μM) trypsin was incubated with different nanomaterials or water as indicated in the text at room temperature (25 °C) before incubation with 2500 μg/mL denatured protein substrate in 20 mM PBS (pH 8.0). Each reaction was digested at 40 °C for 10 min, and then terminated using 0.2 M trichloroacetic acid. The amount of digestion products (short tyrosine-containing peptides) was determined by the Lowry method.[78]

Catalytic activities of chymotrypsin and proteinase K were measured using the same method as described above, except that proteinase K digestion was carried out in 10 mM $CaCl_2$, 50 mM Tris-HCl (pH 7.5).

For visualization of trypsin digestion of casein and decasein, casein was dephosphorylated by FastAP (Fermentas) according to manufacturer's instruction. Reactions were incubated at 40 °C for 3 and 4 min and stopped by addition of 2 X Laemmli buffer. Digestion products and undigested substrates remained in each reaction were separated on 12% SDS-PAGE gels followed by Coomassie Blue stain.

Enzyme Kinetic Analysis. For *v* measurement, digestion reactions were carried out using 20 μg/mL trypsin as described above. Progress curves (initial reaction stage) of each digestion of increasing concentrations of substrates (100, 200, 250, 500, 750, 1250, and 2500 μg/mL) were recorded every 1−15 s (vary depending on [S] and nanomaterial used). Value of *v* was calculated using the equation *v* (μg mL^{-1} min^{-1}) = change in concentration of tyrosine (μg mL^{-1})/elapsed time (min).

Long-term progress curves (over the 0−60 min period) of trypsin digestion reactions were recorded using the same method as described above, except that 2500 μg/mL casein was served as the substrate in all reactions.

Conflict of Interest: The authors declare no competing financial interest.

Acknowledgment. We thank Dr. Zheyong Yu for useful comments and discussions. This work is supported by the National Basic Research Program of China (973 Program, 2012CB932600 and 2011CB911004), NSFC (51132006, 31070707, 91027039, 51002100), the Research Fund for the Doctoral Program of Higher Education of China (20103201120021), CRF project CityU5/CRF/08, and a project funded by the Priority Academic Program Development of Jiangsu Higher Education Institutions (PAPD).

Supporting Information Available: Additional figures. This material is available free of charge *via* the Internet at http://pubs.acs.org.

Note Added after ASAP Publication: After this paper was published online May 17, 2012, corrections were made to Table 2. The corrected version was reposted May 30, 2012.

REFERENCES AND NOTES

1. Howell, J. M. Biocatalysis. *Nat. Biotechnol.* **1983**, *1*, 101–101.
2. Kirk, O.; Borchert, T. V.; Fuglsang, C. C. Industrial Enzyme Applications. *Curr. Opin. Biotechnol.* **2002**, *13*, 345–351.
3. You, C.-C.; Agasti, S. S.; De, M.; Knapp, M. J.; Rotello, V. M. Modulation of the Catalytic Behavior of α-Chymotrypsin at Monolayer-Protected Nanoparticle Surfaces. *J. Am. Chem. Soc.* **2006**, *128*, 14612–14618.
4. Phadtare, S.; Kumar, A.; Vinod, V. P.; Dash, C.; Palaskar, D. V.; Rao, M.; Shukla, P. G.; Sivaram, S.; Sastry, M. Direct Assembly of Gold Nanoparticle "Shell" on Polyurethane Microsphere "Core" and Their Application as Enzyme Immobilization Templates. *Chem. Mater.* **2003**, *15*, 1944–1949.
5. Lv, M.; Zhu, E.; Su, Y.; Li, Q.; Li, W.; Zhao, Y.; Huang, Q. Trypsin-Gold Nanoparticle Conjugates: Binding, Enzymatic Activity, and Stability. *Prep. Biochem. Biotechnol.* **2009**, *39*, 429–438.
6. Konwarh, R.; Karak, N.; Rai, S. K.; Mukherjee, A. K. Polymer-Assisted Iron Oxide Magnetic Nanoparticle Immobilized Keratinase. *Nanotechnology* **2009**, *20*, 225107.
7. Li, J.; Wang, J.; Gavalas, V. G.; Atwood, D. A.; Bachas, L. G. Alumina-Pepsin Hybrid Nanoparticles with Orientation-Specific Enzyme Coupling. *Nano Lett.* **2002**, *3*, 55–58.
8. Yang, Z.; Si, S.; Zhang, C. Study on the Activity and Stability of Urease Immobilized onto Nanoporous Alumina Membranes. *Microporous Mesoporous Mater.* **2008**, *111*, 359–366.
9. Lee, C.-H.; Lin, T.-S.; Mou, C.-Y. Mesoporous Materials for Encapsulating Enzymes. *Nano Today* **2009**, *4*, 165–179.
10. Lei, C.; Shin, Y.; Liu, J.; Ackerman, E. J. Entrapping Enzyme in a Functionalized Nanoporous Support. *J. Am. Chem. Soc.* **2002**, *124*, 11242–11243.
11. Luckarift, H. R.; Spain, J. C.; Naik, R. R.; Stone, M. O. Enzyme Immobilization in a Biomimetic Silica Support. *Nat. Biotechnol.* **2004**, *22*, 211–213.
12. Kim, J.; Grate, J. W.; Wang, P. Nanostructures for Enzyme Stabilization. *Chem. Eng. Sci.* **2006**, *61*, 1017–1026.
13. Lee, S. Y.; Lee, J.; Chang, J. H.; Lee, J. H. Inorganic Nanomaterial-Based Biocatalysts. *BMB Rep.* **2011**, *44*, 77–86.
14. Wang, Y.; Li, Z.; Wang, J.; Li, J.; Lin, Y. Graphene and Graphene Oxide: Biofunctionalization and Applications in Biotechnology. *Trends Biotechnol.* **2011**, *29*, 205–12.
15. Feng, L.; Liu, Z. Graphene in Biomedicine: Opportunities and Challenges. *Nanomedicine* **2011**, *6*, 317–324.
16. Yan, L.; Zheng, Y. B.; Zhao, F.; Li, S.; Gao, X.; Xu, B.; Weiss, P. S.; Zhao, Y. Chemistry and Physics of a Single Atomic Layer: Strategies and Challenges for Functionalization of Graphene and Graphene-Based Materials. *Chem. Soc. Rev.* **2012**, *41*, 97–114.
17. Loh, K. P.; Bao, Q.; Eda, G.; Chhowalla, M. Graphene Oxide as a Chemically Tunable Platform for Optical Applications. *Nat. Chem.* **2010**, *2*, 1015–1024.
18. Feng, L.; Zhang, S.; Liu, Z. Graphene Based Gene Transfection. *Nanoscale* **2011**, *3*, 1252–1257.

19. Liu, Z.; Robinson, J. T.; Sun, X. M.; Dai, H. J. PEGylated Nanographene Oxide for Delivery of Water-Insoluble Cancer Drugs. *J. Am. Chem. Soc.* **2008**, *130*, 10876–10877.
20. Zhang, L.; Lu, Z.; Zhao, Q.; Huang, J.; Shen, H.; Zhang, Z. Enhanced Chemotherapy Efficacy by Sequential Delivery of siRNA and Anticancer Drugs Using PEI-Grafted Graphene Oxide. *Small* **2011**, *7*, 460–464.
21. Zhang, L.; Xia, J.; Zhao, Q.; Liu, L.; Zhang, Z. Functional Graphene Oxide as a Nanocarrier for Controlled Loading and Targeted Delivery of Mixed Anticancer Drugs. *Small* **2010**, *6*, 537–544.
22. Yang, X.; Zhang, X.; Liu, Z.; Ma, Y.; Huang, Y.; Chen, Y. High-Efficiency Loading and Controlled Release of Doxorubicin Hydrochloride on Graphene Oxide. *J. Phys. Chem. C* **2008**, *112*, 17554–17558.
23. Chen, B.; Liu, M.; Zhang, L.; Huang, J.; Yao, J.; Zhang, Z. Polyethylenimine-Functionalized Graphene Oxide as an Efficient Gene Delivery Vector. *J. Mater. Chem.* **2011**, *21*, 7736–7741.
24. Bao, H.; Pan, Y.; Ping, Y.; Sahoo, N. G.; Wu, T.; Li, L.; Li, J.; Gan, L. H. Chitosan-Functionalized Graphene Oxide as a Nanocarrier for Drug and Gene Delivery. *Small* **2011**, *7*, 1569–1578.
25. Sun, X.; Liu, Z.; Welsher, K.; Robinson, J. T.; Goodwin, A.; Zaric, S.; Dai, H. Nano-Graphene Oxide for Cellular Imaging and Drug Delivery. *Nano Res.* **2008**, *1*, 203–212.
26. Peng, C.; Hu, W.; Zhou, Y.; Fan, C.; Huang, Q. Intracellular Imaging with a Graphene-Based Fluorescent Probe. *Small* **2010**, *6*, 1686–1692.
27. Liu, Z.; Robinson, J. T.; Tabakman, S. M.; Yang, K.; Dai, H. Carbon Materials for Drug Delivery & Cancer Therapy. *Mater. Today* **2011**, *14*, 316–323.
28. Dong, H.; Zhao, Z.; Wen, H.; Li, Y.; Guo, F.; Shen, A.; Pilger, F.; Lin, C.; Shi, D. Poly(ethylene glycol) Conjugated Nano-Graphene Oxide for Photodynamic Therapy. *Sci. China Chem.* **2010**, *53*, 2265–2271.
29. Markovic, Z. M.; Harhaji-Trajkovic, L. M.; Todorovic-Markovic, B. M.; Kepic, D. P.; Arsikin, K. M.; Jovanovic, S. P.; Pantovic, A. C.; Dramicanin, M. D.; Trajkovic, V. S. *In vitro* Comparison of the Photothermal Anticancer Activity of Graphene Nanoparticles and Carbon Nanotubes. *Biomaterials* **2011**, *32*, 1121–1129.
30. Peng Huang, C. X.; Lin, J.; Wang, C.; Wang, X.; Zhang, C.; Zhou, X.; Guo, S.; Cui, D. Folic Acid-Conjugated Graphene Oxide Loaded with Photosensitizers for Targeting Photodynamic Therapy. *Theranostics* **2011**, *1*, 240–250.
31. Robinson, J. T.; Tabakman, S. M.; Liang, Y.; Wang, H.; Sanchez Casalongue, H.; Vinh, D.; Dai, H. Ultrasmall Reduced Graphene Oxide with High Near-Infrared Absorbance for Photothermal Therapy. *J. Am. Chem. Soc.* **2011**, *133*, 6825–6831.
32. Tian, B.; Wang, C.; Zhang, S.; Feng, L.; Liu, Z. Photothermally Enhanced Photodynamic Therapy Delivered by Nano-Graphene Oxide. *ACS Nano* **2011**, *5*, 7000–7009.
33. Yang, K.; Zhang, S.; Zhang, G.; Sun, X.; Lee, S.-T.; Liu, Z. Graphene in Mice: Ultrahigh *In Vivo* Tumor Uptake and Efficient Photothermal Therapy. *Nano Lett.* **2010**, *10*, 3318–3323.
34. Zhang, W.; Guo, Z.; Huang, D.; Liu, Z.; Guo, X.; Zhong, H. Synergistic Effect of Chemo-Photothermal Therapy Using PEGylated Graphene Oxide. *Biomaterials* **2011**, *32*, 8555–8561.
35. Yang, K.; Wan, J.; Zhang, S.; Tian, B.; Zhang, Y.; Liu, Z. The Influence of Surface Chemistry and Size of Nanoscale Graphene Oxide on Photothermal Therapy of Cancer Using Ultra-Low Laser Power. *Biomaterials* **2012**, *33*, 2206–2214.
36. Huang, X.; Yin, Z.; Wu, S.; Qi, X.; He, Q.; Zhang, Q.; Yan, Q.; Boey, F.; Zhang, H. Graphene-Based Materials: Synthesis, Characterization, Properties, and Applications. *Small* **2011**, *7*, 1876–1902.
37. Balapanuru, J.; Yang, J.-X.; Xiao, S.; Bao, Q.; Jahan, M.; Polavarapu, L.; Wei, J.; Xu, Q.-H.; Loh, K. P. A Graphene Oxide−Organic Dye Ionic Complex with DNA-Sensing and Optical-Limiting Properties. *Angew. Chem., Int. Ed.* **2010**, *122*, 6699–6703.
38. Kuila, T.; Bose, S.; Khanra, P.; Mishra, A. K.; Kim, N. H.; Lee, J. H. Recent Advances in Graphene-Based Biosensors. *Biosens. Bioelectron.* **2011**, *26*, 4637–4648.
39. Shao, Y.; Wang, J.; Wu, H.; Liu, J.; Aksay, I. A.; Lin, Y. Graphene Based Electrochemical Sensors and Biosensors: A Review. *Electroanalysis* **2010**, *22*, 1027–1036.
40. Wang, Z.; Zhang, J.; Chen, P.; Zhou, X.; Yang, Y.; Wu, S.; Niu, L.; Han, Y.; Wang, L.; Chen, P.; *et al.* Label-Free, Electrochemical Detection of Methicillin-Resistant *Staphylococcus aureus* DNA with Reduced Graphene Oxide-Modified Electrodes. *Biosens. Bioelectron.* **2011**, *26*, 3881–3886.
41. Liu, Y.; Dong, X.; Chen, P. Biological and Chemical Sensors Based on Graphene Materials. *Chem. Soc. Rev.* **2012**, *41*, 2283–2307.
42. Hu, W.; Peng, C.; Luo, W.; Lv, M.; Li, X.; Li, D.; Huang, Q.; Fan, C. Graphene-Based Antibacterial Paper. *ACS Nano* **2010**, *4*, 4317–4323.
43. Xu, W.-P.; Zhang, L.-C.; Li, J.-P.; Lu, Y.; Li, H.-H.; Ma, Y.-N.; Wang, W.-D.; Yu, S.-H. Facile Synthesis of Silver@Graphene Oxide Nanocomposites and Their Enhanced Antibacterial Properties. *J. Mater. Chem.* **2011**, *21*, 4593–4597.
44. Duch, M. C.; Budinger, G. R.; Liang, Y. T.; Soberanes, S.; Urich, D.; Chiarella, S. E.; Campochiaro, L. A.; Gonzalez, A.; Chandel, N. S.; Hersam, M. C.; *et al.* Minimizing Oxidation and Stable Nanoscale Dispersion Improves the Biocompatibility of Graphene in the Lung. *Nano Lett.* **2011**, *11*, 5201–5207.
45. Yang, K.; Wan, J.; Zhang, S.; Zhang, Y.; Lee, S. T.; Liu, Z. *In Vivo* Pharmacokinetics, Long-Term Biodistribution, and Toxicology of PEGylated Graphene in Mice. *ACS Nano* **2011**, *5*, 516–522.
46. Hu, W.; Peng, C.; Lv, M.; Li, X.; Zhang, Y.; Chen, N.; Fan, C.; Huang, Q. Protein Corona-Mediated Mitigation of Cytotoxicity of Graphene Oxide. *ACS Nano* **2011**, *5*, 3693–3700.
47. Ruiz, O. N.; Fernando, K. A.; Wang, B.; Brown, N. A.; Luo, P. G.; McNamara, N. D.; Vangsness, M.; Sun, Y. P.; Bunker, C. E. Graphene Oxide: A Nonspecific Enhancer of Cellular Growth. *ACS Nano* **2011**, *5*, 8100–8107.
48. Yan, L.; Zhao, F.; Li, S.; Hu, Z.; Zhao, Y. Low-Toxic and Safe Nanomaterials by Surface-Chemical Design, Carbon Nanotubes, Fullerenes, Metallofullerenes, and Graphenes. *Nanoscale* **2011**, *3*, 362–382.
49. Alwarappan, S.; Liu, C.; Kumar, A.; Li, C.-Z. Enzyme-Doped Graphene Nanosheets for Enhanced Glucose Biosensing. *J. Phys. Chem. C* **2010**, *114*, 12920–12924.
50. Liu, Y.; Yu, D.; Zeng, C.; Miao, Z.; Dai, L. Biocompatible Graphene Oxide-Based Glucose Biosensors. *Langmuir* **2010**, *26*, 6158–6160.
51. Kang, X.; Wang, J.; Wu, H.; Aksay, I. A.; Liu, J.; Lin, Y. Glucose Oxidase-Graphene-Chitosan Modified Electrode for Direct Electrochemistry and Glucose Sensing. *Biosens. Bioelectron.* **2009**, *25*, 901–905.
52. Shan, C.; Yang, H.; Song, J.; Han, D.; Ivaska, A.; Niu, L. Direct Electrochemistry of Glucose Oxidase and Biosensing for Glucose Based on Graphene. *Anal. Chem.* **2009**, *81*, 2378–2382.
53. Zhang, J.; Zhang, F.; Yang, H.; Huang, X.; Liu, H.; Zhang, J.; Guo, S. Graphene Oxide as a Matrix for Enzyme Immobilization. *Langmuir* **2010**, *26*, 6083–6085.
54. Zeng, Q.; Cheng, J.; Tang, L.; Liu, X.; Liu, Y.; Li, J.; Jiang, J. Self-Assembled Graphene−Enzyme Hierarchical Nanostructures for Electrochemical Biosensing. *Adv. Funct. Mater.* **2010**, *20*, 3366–3372.
55. Zhang, F.; Zheng, B.; Zhang, J.; Huang, X.; Liu, H.; Guo, S.; Zhang, J. Horseradish Peroxidase Immobilized on Graphene Oxide: Physical Properties and Applications in Phenolic Compound Removal. *J. Phys. Chem. C* **2010**, *114*, 8469–8473.
56. Lu, Q.; Dong, X.; Li, L.-J.; Hu, X. Direct Electrochemistry-Based Hydrogen Peroxide Biosensor Formed from Single-Layer Graphene Nanoplatelet-Enzyme Composite Film. *Talanta* **2010**, *82*, 1344–1348.
57. Zhang, Q.; Qiao, Y.; Zhang, L.; Wu, S.; Zhou, H.; Xu, J.; Song, X.-M. Direct Electrochemistry and Electrocatalysis of

Horseradish Peroxidase Immobilized on Water Soluble Sulfonated Graphene Film *via* Self-Assembly. *Electroanalysis* **2011**, *23*, 900–906.
58. Huang, C.; Bai, H.; Li, C.; Shi, G. A Graphene Oxide/Hemoglobin Composite Hydrogel for Enzymatic Catalysis in Organic Solvents. *Chem. Commun.* **2011**, *47*, 4962–4964.
59. De, M.; Chou, S. S.; Dravid, V. P. Graphene Oxide as an Enzyme Inhibitor: Modulation of Activity of α-Chymotrypsin. *J. Am. Chem. Soc.* **2011**, *133*, 17524–17527.
60. Stroud, R. M.; Kay, L. M.; Dickerson, R. E. The Structure of Bovine Trypsin: Electron Density Maps of the Inhibited Enzyme at 5 Å and at 2·7 Å Resolution. *J. Mol. Biol.* **1974**, *83*, 185–208.
61. Blow, D. M.; Birktoft, J. J.; Hartley, B. S. Role of a Buried Acid Group in the Mechanism of Action of Chymotrypsin. *Nature* **1969**, *221*, 337–340.
62. Betzel, C.; Pal, G. P.; Saenger, W. Three-Dimensional Structure of Proteinase K at 0.15-nm Resolution. *Eur. J. Biochem.* **1988**, *178*, 155–171.
63. Modler, H. W. Functional Properties of Nonfat Dairy Ingredients - A Review. Modification of Products Containing Casein. *J. Dairy Sci.* **1985**, *68*, 2195–2205.
64. Laemmli, U. K. Cleavage of Structural Proteins During the Assembly of the Head of Bacteriophage T4. *Nature* **1970**, *227*, 680–685.
65. Hedstrom, L. Serine Protease Mechanism and Specificity. *Chem. Rev.* **2002**, *102*, 4501–4523.
66. De Haen, C.; Neurath, H.; Teller, D. C. The Phylogeny of Trypsin-Related Serine Proteases and Their Zymogens. New Methods for the Investigation of Distant Evolutionary Relationships. *J. Mol. Biol.* **1975**, *92*, 225–259.
67. Ma, W.; Tang, C.; Lai, L. Specificity of Trypsin and Chymotrypsin: Loop-Motion-Controlled Dynamic Correlation as a Determinant. *Biophys. J.* **2005**, *89*, 1183–1193.
68. Reed, M. C.; Lieb, A.; Nijhout, H. F. The Biological Significance of Substrate Inhibition: A Mechanism with Diverse Functions. *Bioessays* **2010**, *32*, 422–429.
69. Chaplin, M. Fundamentals of Enzyme Kinetics. In *Enzyme Technology*, Chaplin, M., Bucke, C., Eds.; Cambridge University: Cambridge, 1990; pp 27−35.
70. Graf, L.; Jancso, A.; Szilagyi., L.; Hegyi, G.; Pinttr, K.; Naray-Szabo, G.; Hepp, J.; Medzihardszky, K.; Rutter, W. J. Electrostatic Complementarity within the Substrate-Binding Pocket of Trypsin. *Proc. Natl. Acad. Sci. U.S.A.* **1988**, *85*, 4961–4965.
71. Olsen, J. V.; Ong, S.-E.; Mann, M. Trypsin Cleaves Exclusively C-Terminal to Arginine and Lysine Residues. *Mol. Cell. Proteomics* **2004**, *3*, 608–614.
72. Oda, Y.; Nagasu, T.; Chait, B. T. Enrichment Analysis of Phosphorylated Proteins as a Tool for Probing the Phosphoproteome. *Nat. Biotechnol.* **2001**, *19*, 379–382.
73. Ozlu, N.; Akten, B.; Timm, W.; Haseley, N.; Steen, H.; Steen, J. A. J. Phosphoproteomics. *Wiley Interdiscip. Rev.* **2010**, *2*, 255–276.
74. Lemeer, S.; Heck, A. J. R. The Phosphoproteomics Data Explosion. *Curr. Opin. Chem. Biol.* **2009**, *13*, 414–420.
75. Manning, G.; Whyte, D. B.; Martinez, R.; Hunter, T.; Sudarsanam, S. The Protein Kinase Complement of the Human Genome. *Science* **2002**, *298*, 1912–1934.
76. Hummers, W. S.; Offeman, R. E. Preparation of Graphitic Oxide. *J. Am. Chem. Soc.* **1958**, *80*, 1339.
77. Hummel, B. C. W. A Modified Spectrophotometric Determination of Chymotrypsin, Trypsin, and Thrombin. *Can. J. Biochem. Physiol.* **1959**, *37*, 1393–1399.
78. Lowry, O. H.; Rosebrough, N. J.; Farr, A. L.; Randall, R. J. Protein Measurement with the Folin Phenol Reagent *J. Biol. Chem.* **1951**, *193*, 265–275.